Hyperfine quenching of the metastable $^3P_{0,2}$ states in divalent atoms

Sergey G. Porsev and Andrei Derevianko
Physics Department, University of Nevada, Reno, Nevada 89557-0058, USA
and Petersburg Nuclear Physics Institute, Gatchina, Leningrad District, 188300, Russia
(Received 1 December 2003; published 7 April 2004)

Hyperfine quenching rates of the lowest-energy metastable $^3P_0$ and $^3P_2$ states of Mg, Ca, Sr, and Yb atoms are computed. The calculations are carried out using *ab initio* relativistic many-body methods. The computed lifetimes may be useful for designing novel ultraprecise optical clocks and trapping experiments with the $^3P_2$ fermionic isotopes. The resulting natural widths of the $^3P_0$-$^1S_0$ clock transition are 0.44 mHz for ^{25}Mg, 2.2 mHz for ^{43}Ca, 7.6 mHz for ^{87}Sr, 43.5 mHz for ^{171}Yb, and 38.5 mHz for ^{173}Yb. Compared to the bosonic isotopes, the lifetime of the $^3P_2$ states in fermionic isotopes is noticeably shortened by the hyperfine quenching but still remains long enough for trapping experiments.

DOI: 10.1103/PhysRevA.69.042506 PACS number(s): 32.70.Cs, 32.10.Fn, 31.15.Ar

I. INTRODUCTION

This work is motivated by emerging experiments with cold divalent atoms Mg, Ca, Sr, and Yb [1]. For example, the recently attained Bose-Einstein condensate of the ground-state Yb [2] may offer new insights into the physics of degenerate quantum gases due to a vast number of available isotopes and relative simplicity of molecular potentials. As to the $^3P_2$ metastable states (see Fig. 1), it was realized that the nonscalar nature of the $^3P_2$ states may be used to overcome the unfeasibility of magnetic trapping of the spherically symmetric $^1S_0$ ground states [3–6]. Knowing radiative lifetimes of the other $^3P_0$ metastable states is required in developing the next generation of ultraprecise optical atomic clocks [7–10]. Here the clockwork is based on cold atoms confined to sites of an engineered optical lattice. The lifetime determines the natural width of the clock transition between the ground and the $^3P_0$ state.

For all *bosonic* isotopes of Mg, Ca, Sr, and Yb, the nuclear spin I vanishes and these isotopes lack hyperfine structure. For bosonic isotopes the $^3P_0$ state may decay only via very weak multiphoton (e.g., $E1$-$M1$) transitions. However, for *fermionic* isotopes (Table I), $I\neq 0$, a new radiative decay channel becomes available due to the hyperfine interaction (HFI). The HFI, although small, admixes atomic levels of the total angular momentum $J=1$ thus opening an electric-dipole branch to the ground state. The resulting HFI-induced $E1$ decays do determine the lifetimes of the $^3P_0$ states. As to the $^3P_2$ states, here the single-photon decays are allowed, but being of non-$E1$ character, are very weak. The lifetimes are long and range from 15 s for Yb to 2 h for Ca [11,12]. As we demonstrate here, depending on an isotope, the hyperfine quenching of the $^3P_2$ states is either comparable to or is much faster than the small non-$E1$ rates.

A detailed theoretical analysis of the hyperfine quenching has been limited so far to astrophysically important He, Be, and Mg and their isoelectronic sequences [13–16]. The hyperfine quenching of the $^3P_0$ states of Sr and Yb has been estimated in Refs. [7,10]. Here we carry out *ab initio* relativistic many-body atomic structure calculations to extend and refine these previous studies. We find that the resulting natural widths of the $^3P_0-{}^1S_0$ clock transition are 0.44 mHz for ^{25}Mg, 2.2 mHz for ^{43}Ca, 7.6 mHz for ^{87}Sr, 43.5 mHz for ^{171}Yb, and 38.5 mHz for ^{173}Yb. Compared to the bosonic isotopes, the lifetime of the $^3P_2$ states in fermionic isotopes is noticeably shortened by the hyperfine quenching but still remains long enough for trapping experiments.

The paper is organized as follows. First, in Sec. II we derive the hyperfine quenching rates using perturbation theory. The solution of many-body atomic problem and numerical details are given in Sec. III. Finally, we present the results, compare with the previous calculations, and draw the conclusions in Sec. IV. Unless noted otherwise, atomic units ($\hbar=|e|=m_e\equiv 1$) are used throughout.

II. DERIVATION OF HYPERFINE QUENCHING RATES

In the presence of nuclear moments, the total electronic angular momentum J no longer remains a good quantum number. The atomic energy levels are characterized instead by the total angular momentum $\mathbf{F}=\mathbf{J}+\mathbf{I}$. Nevertheless, the coupling of the electronic and the nuclear momenta is small and in this section we employ the first-order perturbation theory in the magnetic-dipole hyperfine interaction to compute the modified atomic wave functions of the $^3P_{0;2}$ levels.

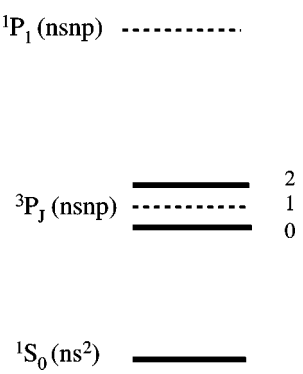

FIG. 1. Lowest-lying energy levels of Mg ($n=3$), Ca ($n=4$), Sr ($n=5$), and Yb ($n=6$), relevant to the radiative decay of the $nsnp$ $^3P_{0,2}$ states. The hyperfine quenching predominantly is caused by the admixture of the $nsnp$ $^3P_1$ and $nsnp$ $^1P_1$ states.

TABLE I. Nuclear parameters of the stable fermionic isotopes of Mg, Ca, Sr, and Yb. Here I are the nuclear spins, μ/μ_N are the nuclear magnetic moments expressed in units of the nuclear magneton μ_N, and Q are the nuclear quadrupole moments expressed in barns.

Isotope	I	μ/μ_N	Q
^{25}Mg	5/2	−0.85546	0.1994(20)
^{43}Ca	7/2	−1.31727	−0.0408(8)
^{87}Sr	9/2	−1.09283	0.335(20)
^{171}Yb	1/2	0.4919	0
^{173}Yb	5/2	−0.6776	2.800(40)

With these perturbed wave functions the hyperfine quenching rates are obtained with the conventional Fermi golden rule.

Before proceeding with the outlined derivation, we note that in this problem there are two types of perturbations: the hyperfine interaction and the interaction with the electromagnetic field. Here we treat the HFI as the dominant interaction, determine the hyperfine structure first, and as the next step compute the lifetimes. This approach is valid as long as the radiative width of the $^3P_1$ level is much smaller than the fine-structure intervals between the components of the ^3P_J multiplet [14]. We verified that this inequality holds for all the atoms under consideration.

We develop the formalism in terms of the hyperfine states $|\gamma(IJ)FM_F\rangle$. Here the angular momenta I and J are conventionally coupled to produce a state of definite total momentum F and its projection M_F, and γ encapsulates all other atomic quantum numbers. In the first order of perturbation theory in the hyperfine interaction, $H_{\rm HFI}$, the correction to the hyperfine sublevel $|\gamma(IJ)FM_F\rangle$ of the metastable state $|\gamma J\rangle$ reads

$$|\gamma(IJ)FM_F\rangle^{(1)} = \sum_{\gamma' J'} |\gamma'(IJ')FM_F\rangle \times \frac{\langle\gamma'(IJ')FM_F|H_{\rm HFI}|\gamma(IJ)FM_F\rangle}{E(\gamma' J') - E(\gamma J)}, \quad (1)$$

where $E(\gamma J)$ are the energies of atomic states. In the above expression, we have taken into account that $H_{\rm HFI}$ is a scalar, so the total angular momentum F and its projection M_F are conserved. In general, the hyperfine coupling Hamiltonian $H_{\rm HFI}$ may be represented as a sum over multipole nuclear moments $\mathcal{M}^{(k)}_\lambda$ of rank k combined with the even-parity electronic coupling operators $\mathcal{T}^{(k)}_\lambda$ of the same rank so that the total interaction is rotationally and P invariant,

$$H_{\rm HFI} = \sum_k (\mathcal{M}^{(k)}\mathcal{T}^{(k)}).$$

In the following we limit the discussion to the contributions from the nuclear magnetic-dipole ($k=1$) and electric-quadrupole ($k=2$) moments. The conventionally defined nuclear moments are related to the tensors $\mathcal{M}^{(k)}_\lambda$ as $\mu \equiv \langle IM_I=I|\mathcal{M}^{(1)}_0|IM_I=I\rangle$ and $Q \equiv 2\langle IM_I=I|\mathcal{M}^{(2)}_0|IM_I=I\rangle$. We list the moments for the isotopes of interest in Table I. Note that the quadrupole moment of ^{171}Yb vanishes, since the nuclear spin $I=1/2$ for this isotope.

Using the Wigner-Eckart theorem, the matrix element of the hyperfine interaction in Eq. (1) may be simplified to

$$\langle\gamma'(IJ');FM_F|H_{\rm HFI}|\gamma(IJ);FM_F\rangle = \delta_{FF'}\delta_{M_F M'_F}(-1)^{I+J'+F}\sum_k \langle I\|M^{(k)}\|I\rangle\langle n'J'\|T^{(k)}\|nJ\rangle \times \begin{Bmatrix} I & I & k \\ J & J' & F \end{Bmatrix}. \quad (2)$$

Given the correction to the wave function, Eq. (1), we derive the hyperfine quenching rate using the standard formalism of the Fermi golden rule. The rate of spontaneous emission $(a\to b)$ for an electric-dipole radiation is

$$A_{a\to b} = \frac{4\alpha^3}{3}\omega^3_{ab}|\langle a|\mathbf{D}|b\rangle|^2, \quad (3)$$

where $\alpha\approx 1/137$ is the fine-structure constant, $\omega_{ab}=E_a-E_b$ is the transition frequency, and $\mathbf{D}$ is the electric-dipole operator. Summing over all possible F_b and magnetic quantum numbers M_b of the final state, while disregarding small F-dependent energy correction, one obtains

$$A_{a\to b} = \frac{4\alpha^3}{3}\omega^3_{ab}\frac{1}{2F_a+1}\sum_{F_b}|\langle a\|D\|b\rangle|^2. \quad (4)$$

For the case at hand, the initial state is the HFI-perturbed $nsnp\ ^3P_J, (J\neq 1)$ state, and the final state is the ground $ns^2\ ^1S_0$ state. Taking into account Eq. (1), we arrive at the hyperfine quenching rate as

$$A_{\rm HFI}(nsnp\ ^3P_J; F\to ns^2\ ^1S_0) = \frac{4\alpha^3}{9}\omega^3_J\left|\sum_k S_k\right|^2, \quad (5)$$

with $\omega_J=E(nsnp\ ^3P_J)-E(ns^2\ ^1S_0)$ and the sums S_k defined as

$$S_k = \langle I\|\mathcal{M}^{(k)}\|I\rangle\sum_{\gamma',J'}\begin{Bmatrix} I & I & k \\ J & J' & F \end{Bmatrix} \times \frac{\langle ns^2\ ^1S_0\|D\|\gamma' J'\rangle\langle\gamma' J'\|T^{(k)}\|nsnp\ ^3P_J\rangle}{E(\gamma' J') - E(nsnp\ ^3P_J)}. \quad (6)$$

Note that due to the electric-dipole selection rules, $J'=1$. Due to this restriction, in a particular case of the $nsnp\ ^3P_0$ states only the magnetic ($k=1$) HFI coupling causes the $E1$ transitions and Eqs. (5) and (6) are simplified to

$$A_{\rm HFI}(nsnp\ ^3P_0;F=I\to ns^2\ ^1S_0)=\frac{4\alpha^3}{27}\omega_0^3\mu^2\frac{I+1}{I}\left|\sum_{\gamma'}\frac{\langle ns^2\ ^1S_0\|D\|\gamma' J'=1\rangle\langle\gamma' J'=1\|\mathcal{T}^{(1)}\|nsnp\ ^3P_0\rangle}{E(\gamma' J'=1)-E(nsnp\ ^3P_0)}\right|^2. \quad (7)$$

For the case of $nsnp\ ^3P_2$ state we restrict our consideration by the first two terms in the sum over k in Eq. (5). In the following section we carry out *ab initio* relativistic many-body calculations of the derived hyperfine quenching rates.

III. SOLVING ATOMIC MANY-BODY PROBLEM

The *ab initio* relativistic atomic-structure calculations employed here are similar to computations of electric-dipole amplitudes for the alkaline-earth-metal atoms [17] and hyperfine structure constants and electric-dipole amplitudes for ytterbium [11,18]. Here we only briefly recapitulate the main features of this method. We consider Mg, Ca, Sr, and Yb as atoms with two valence electrons outside the closed-shell cores. Strong repulsion between the two valence electrons is treated nonperturbatively using the configuration-interaction (CI) method. The core-valence and core-core correlations are taken into account with the help of the many-body perturbation theory (MBPT) method. In the following we refer to this combined approach as the CI+MBPT method [19].

In the CI+MBPT approach, the energies and the wave functions are determined from the eigenvalue equation in the model space of the valence electrons

$$H_{\rm eff}(E_p)\ |\Phi_p\rangle=E_p\ |\Phi_p\rangle, \quad (8)$$

where the effective Hamiltonian is defined as

$$H_{\rm eff}(E)=H_{\rm FC}+\Sigma(E). \quad (9)$$

Here $H_{\rm FC}$ is the relativistic two-electron Hamiltonian in the frozen-core approximation and $\Sigma(E)$ is the energy-dependent core-polarization correction. The all-order operator $\Sigma(E)$ completely accounts for the second-order correlation correction to the energies. The omitted diagrams in higher orders may be accounted for indirectly by adjusting the effective Hamiltonian [17,20]. Namely, one introduces an energy shift δ and replaces $\Sigma(E)$ with $\Sigma(E-\delta)$. The parameter δ is determined semiempirically from a fit of the resulting theoretical energy levels to experimental spectrum.

Using the effective Hamiltonian we find the wave functions of the ground and the ^3P_J states. Further we apply the technique of effective all-order (dressed) operators to calculations of the matrix elements. Technically, we employ the random-phase approximation (RPA). The RPA sequence of diagrams describes a shielding of externally applied field by the core electrons. This is the level of approximation employed here for electric-dipole matrix elements. The hyperfine, $\mathcal{T}^{(1)}$ and $\mathcal{T}^{(2)}$, matrix elements required more sophisticated approach: for these operators we additionally incorporated smaller corrections (the details can be found in Ref. [18]). For the heaviest and more computationally demanding Yb, the corrections to the effective hyperfine operator tend to cancel [18], and we have simplified the calculations for Yb by using the bare $\mathcal{T}^{(1)}$ operator.

To demonstrate the quality of the constructed wave functions and the accuracy of the effective-operator approach, in Table II we present the calculated magnetic-dipole hyperfine structure constants A for the $^3P_{1,2}$ states. These constants are expressed in terms of expectation values of $H_{\rm HFI}$. As seen from the Table II the differences between the calculated and the experimental values, even for heavy Yb, do not exceed 1%.

Further the sums S_k, Eq. (6), are computed in the framework of Sternheimer-Dalgarno-Lewis method [27,28]. At the heart of this method is the recasting of the sums S_k in the form

$$S_k=\langle I\|\mathcal{M}^{(k)}\|I\rangle\begin{Bmatrix} I & I & k\\ J & 1 & F\end{Bmatrix}\langle\delta\Psi\|\mathcal{T}^{(k)}_{\rm eff}\|nsnp\ ^3P_J\rangle, \quad (10)$$

where $|\delta\Psi\rangle$ satisfies the inhomogeneous Schrodinger equation

$$[H_{\rm eff}-E(nsnp\ ^3P_J)]|\delta\Psi\rangle=D_{\rm eff}|ns^2\ ^1S_0\rangle. \quad (11)$$

It is worth noting that because the effective operators act in the valence model space, the $|\delta\Psi\rangle$ solution encompasses only the excitations of the valence electrons to higher valence states. The unaccounted for core excitations involve

TABLE II. Magnetic-dipole hyperfine structure constants A for the $nsnp\ ^3P_1$ and $nsnp\ ^3P_2$ states. The computed values are compared with the experimental data.

		$A(^3P_1^0)$ (MHz)	$A(^3P_2^0)$ (MHz)
^{25}Mg	This work	−146.1	−129.7
	Experiment	−144.977(5)[a]	−128.445(5)[a]
^{43}Ca	This work	−199.2	−173.1
	Experiment	−198.890(1)[b]	−171.962(2)[c]
^{87}Sr	This work	−258.7	−211.4
	Experiment	−260.083(5)[d]	−212.765(1)[d]
^{171}Yb	This work	3964	2704
	Experiment	3957.97(47)[e]	2677.6[f]
^{173}Yb	This work	−1092	−745
	Experiment	−1094.20(60)[e]	−737.7[f]

[a]Lurio [21].
[b]Arnold *et al.* [22].
[c]Grundevik *et al.* [23].
[d]Heider and Brink [24].
[e]Clark *et al.* [25].
[f]Budick and Snir [26].

TABLE III. Sums S_k for the metastable $^3P_0$ and $^3P_2$ states for different total angular momenta F are presented. The values are given in atomic units.

	F	$S_1, nsnp\ ^3P_0$	$S_1, nsnp\ ^3P_2$	$S_2, nsnp\ ^3P_2$
^{25}Mg	3/2		-5.7×10^{-6}	7.1×10^{-8}
	5/2	8.0×10^{-6}	8.1×10^{-6}	-3.8×10^{-8}
	7/2		-8.4×10^{-6}	-5.2×10^{-8}
^{43}Ca	5/2		2.1×10^{-5}	3.3×10^{-8}
	7/2	-3.1×10^{-5}	-2.7×10^{-5}	-1.3×10^{-8}
	9/2		2.7×10^{-5}	-2.6×10^{-8}
^{87}Sr	7/2		4.3×10^{-5}	-6.0×10^{-7}
	9/2	6.2×10^{-5}	-5.5×10^{-5}	1.9×10^{-7}
	11/2		5.3×10^{-5}	4.9×10^{-7}
^{171}Yb	1/2	-1.2×10^{-4}		
	3/2		-1.3×10^{-4}	
^{173}Yb	3/2		-7.5×10^{-5}	1.1×10^{-5}
	5/2	-1.1×10^{-4}	-1.1×10^{-4}	-5.9×10^{-6}
	7/2		-1.1×10^{-4}	-8.0×10^{-6}

large energy denominators and we disregard their contributions.

IV. RESULTS AND CONCLUSIONS

To reiterate the discussion of the preceding section, we carry out the calculations in several logical steps. First, we solve the CI+MBPT eigenvalue problem (8) and determine the ground and the $nsnp\ ^3P_J$ state wave functions and energies. At the next step, we compute the dressed $E1$-operator $D_{\rm eff}$ and solve the inhomogeneous equation (11). Finally, we calculate the required sums S_k, Eqs. (6) and (10), and determine the hyperfine quenching rates, Eq. (5).

The computed values of the nonvanishing sums S_1 and S_2 for $nsnp\ ^3P_0$ and $nsnp\ ^3P_2$ states for Mg, Ca, Sr, and Yb are presented in Table III. For the $nsnp\ ^3P_0$ the quadrupole sums S_2 vanish due to the selection rules; these sums are not listed. From the table, it is clear that the sums grow larger for heavier atoms. This is due to increasing matrix elements of the hyperfine interaction (see Table II). Further, a direct investigation of the sums shows that the contributions of both $nsnp\ ^3P_1$ and $nsnp\ ^1P_1$ intermediate states are comparable. Qualitatively, the triplet state is separated from the metastable states by a small fine-structure interval, but its $E1$ matrix element with the singlet ground state vanishes nonrelativistically. For the singlet state, the situation is reversed: compared to the triplet contribution, the involved energy denominator is much larger, but the electric-dipole matrix element is allowed.

With the determined values of S_k and Eq. (5), we obtain the hyperfine quenching rates for the metastable $^3P_0$ and $^3P_2$ states. The resulting rates are listed in Table IV. The tabulated decay rates for the $^3P_2$ states require some explanation. First of all, as follows from Eqs. (5) and (6) the quenching rates depend on the total angular momentum F of the hyperfine substate. Although, in general, the total angular momentum F ranges from $|J-I|$ to $J+I$, the $6j$ symbol in Eq. (6) imposes an additional restriction, $|I-1|\leqslant F\leqslant I+1$. This requirement can be tracked to the selection rule for the electric-dipole transition amplitude between the ground state $(J_g=0, F_g=I)$ and the intermediate state which has the same F as the original hyperfine state [see Eq. (1)]. Combined selection rule reads

$$\max(|J-I|,|I-1|)\leqslant F\leqslant \min(J+I,I+1).$$

Keeping this restriction in mind, in Table IV we have listed the quenching rates only for such allowed values of F.

TABLE IV. The hyperfine $E1$-quenching rates for the metastable $^3P_0$ and $^3P_2$ states in s^{-1}. The rates depend on the total angular momentum F. The rates are compared with values by other authors, where available.

Atom	Transition rate	F	This work	Other
^{25}Mg	$A_{\rm HFS}(^3P_0\to{}^1S_0)$	5/2	4.44×10^{-4}	4.2×10^{-4} [a]
	$A_{\rm HFS}(^3P_2\to{}^1S_0)$	3/2	2.25×10^{-4}	1.4×10^{-4} [a]
		5/2	4.65×10^{-4}	2.9×10^{-4} [a]
		7/2	5.02×10^{-4}	3.1×10^{-4} [a]
^{43}Ca	$A_{\rm HFS}(^3P_0\to{}^1S_0)$	7/2	2.22×10^{-3}	
	$A_{\rm HFS}(^3P_2\to{}^1S_0)$	5/2	1.02×10^{-3}	
		7/2	1.81×10^{-3}	
		9/2	1.74×10^{-3}	
^{87}Sr	$A_{\rm HFS}(^3P_0\to{}^1S_0)$	9/2	7.58×10^{-3}	6.3×10^{-3} [b]
	$A_{\rm HFS}(^3P_2\to{}^1S_0)$	7/2	4.01×10^{-3}	
		9/2	6.81×10^{-3}	
		11/2	6.38×10^{-3}	
^{171}Yb	$A_{\rm HFS}(^3P_0\to{}^1S_0)$	1/2	4.35×10^{-2}	5.0×10^{-2} [c]
	$A_{\rm HFS}(^3P_2\to{}^1S_0)$	3/2	9.18×10^{-2}	
^{173}Yb	$A_{\rm HFS}(^3P_0\to{}^1S_0)$	5/2	3.85×10^{-2}	4.3×10^{-2} [c]
	$A_{\rm HFS}(^3P_2\to{}^1S_0)$	3/2	2.14×10^{-2}	
		5/2	5.32×10^{-2}	
		7/2	7.22×10^{-2}	

[a] Garstang [13].
[b] Katori *et al.* [7].
[c] Porsev *et al.* [10].

A relative role of the quadrupole HFI contribution can be illuminated using Table III. The ratio S_2/S_1 for the $nsnp\ ^3P_2$ states is in the order of 0.01 for isotopes of Mg, Ca, and Sr, while for ^{173}Yb it is $\sim$0.1. The enhancement for ^{173}Yb is mostly due to a relatively large nuclear quadrupole moment $Q=2.8$ barn and a small gyromagnetic ratio $g_N=-0.2710$. Our computation shows that the electric-quadrupole hyperfine interaction contributes to the quenching rate at the level of 20 % for ^{173}Yb, at the level of 2–3 % for ^{25}Mg and ^{87}Sr and below 1% for ^{43}Ca. We also remind the reader that for the ^{171}Yb isotope, $I=1/2$ and the nuclear moments beyond the magnetic-dipole moment vanish.

In Table IV we also compare the computed rates with the results from the literature. For Mg the hyperfine quenching rates for the $^3P_2$ state were estimated more than four decades ago by Garstang [13]. Our results are in a reasonable agree-

TABLE V. Comparison of the hyperfine quenching rates (maximum over the hyperfine manifold in Table IV) with the nondipole rates for the $^3P_2$ states. The rates are given in s^{-1}.

Atom	Hyperfine rate, max	Non-$E1$ rate[a]
^{25}Mg	5.02×10^{-4}	4.42×10^{-4}
^{43}Ca	18.1×10^{-4}	1.41×10^{-4}
^{87}Sr	68.1×10^{-4}	9.55×10^{-4}
^{171}Yb	9.18×10^{-2}	6.7×10^{-2}
^{173}Yb	7.22×10^{-2}	6.7×10^{-2}

[a]For Mg, Ca, and Sr the rates are from Ref. [12] and for Yb from Ref. [11].

ment with his values. Certainly, our calculations based on the modern *ab initio* relativistic many-body techniques are more complete. In fact, based on better than 1% accuracy of the *ab initio* hyperfine constants (Table II) and energy levels [17,18] we expect that the computed hyperfine quenching rates are accurate within at least a few percent. Further, in the calculation of the sums S_k, Garstang [13] kept only the two lowest-energy intermediate states $^3P_1$ and $^1P_1$. This author has also employed the following $E1$-matrix elements $|\langle {}^1S_0\|D\|{}^3P_1\rangle|=0.0058$ a.u. and $|\langle {}^1S_0\|D\|{}^1P_1\rangle|=3.46$ a.u., which are smaller than more accurate values [17] of 0.0064(7) a.u. and 4.03(2)a.u., employed here. Our results for ^{87}Sr are in fair agreement with the estimate of Ref. [7]. Previously, we have estimated the quenching rates for Yb isotopes [10] by summing only over the two lowest-energy excited states; the present result should be considered as more accurate.

In Table V the calculated hyperfine quenching rates (maximum over hyperfine manifold) for the $^3P_2$ states are compared with the conventional electromagnetic transition rates. For Mg, Ca, and Sr these rates were calculated in Ref. [12] and are due to $M1$, $M2$, $E2$, and $E3$ multipole transitions. If the hyperfine quenching is allowed for a particular value of F, both rates contribute at a comparable level for Mg and Yb. For Ca and Sr the hyperfine quenching becomes the dominant decay branch and determines the lifetime of the fermionic isotopes.

It is worth mentioning one more process that can potentially lead to a shortening of lifetimes of the metastable states. As demonstrated by Yasuda and Katori [29], the black body radiation (BBR) induced decay rate of the $5s5p\ ^3P_2$ state for Sr is equal to $8.03\times10^{-3}\ s^{-1}$ at 300 K. This decay rate is comparable to the HFI quenching rate computed in this work. A detailed analysis of the BBR effects is beyond the scope of this work. Our order-of-magnitude estimate of the BBR quenching for Mg, Ca, and Yb shows that at room temperature ($T=300$ K) the BBR quenching is negligible compared to the rates caused by the vacuum fluctuations of the electromagnetic field ($T=0$). The reader, however, should be cautioned that the BBR rate strongly depends on the ambient temperature and it may become important, for example, if a hot oven is used as a source of atoms.

To summarize, here we employed relativistic many-body methods to evaluate hyperfine quenching rates for the metastable $^3P_0$ and $^3P_2$ states of Mg, Ca, Sr, and Yb. The tabulated rates may be useful for designing novel ultraprecise optical clocks and trapping experiments with fermionic isotopes of metastable alkaline-earth-metal atoms and Yb. The resulting natural widths of the $^3P_0-{}^1S_0$ clock transition are 0.44 mHz for ^{25}Mg, 2.2 mHz for ^{43}Ca, 7.6 mHz for ^{87}Sr, 43.5 mHz for ^{171}Yb, and 38.5 mHz for ^{173}Yb. Compared to the bosonic isotopes, the lifetime of the $^3P_2$ states in fermionic isotopes is noticeably shortened by the hyperfine quenching but still remains long enough for trapping experiments.

ACKNOWLEDGMENTS

We would like to thank Norval Fortson for bringing this problem to our attention. This work was supported in part by a National Science Foundation grant and by a NIST Precision Measurement grant. The work of S.G.P. was additionally supported by the Russian Foundation for Basic Research under Grants No. 02-02-16837-a and No. 04–02–16345–a.

[1] See, e.g., abstracts of the Second Workshop on Cold Alkaline-Earth Atoms, held September 11-13, 2003 in Copenhagen, Denmark. Abstracts are available from http://www.fys.ku.dk/coldatoms/workshop/workshopgroup2.htm
[2] Y. Takasu, K. Maki, K. Komori, T. Takano, K. Honda, M. Kumakura, T. Yabuzaki, and Y. Takahashi, Phys. Rev. Lett. **91**, 040404 (2003).
[3] H. Katori, T. Ido, Y. Isoya, and M. Kuwata-Gonokami, in Atomic Physics XVII, edited by Ennio Arimondo, Paolo De Natole, and Marrimo Inguscio, AIP Conf. Proc. No. 551 (AIP, Meville, NY, 2001).
[4] S. B. Nagel, C. E. Simien, S. Laha, P. Gupta, V. S. Ashoka, and T. C. Killian, Phys. Rev. A **67**, 011401(R) (2003).
[5] X. Xu, T. H. Loftus, J. L. Hall, A. Gallagher, and J. Ye, J. Opt. Soc. Am. B **20**, 968 (2003).
[6] J. Grünert and A. Hemmerich, Phys. Rev. A **65**, 041401 (2002).
[7] H. Katori, M. Takamoto, V. G. Pal'chikov, and V. D. Ovsiannikov, Phys. Rev. Lett. **91**, 173005 (2003).
[8] I. Courtillot, A. Quessada, R. P. Kovacich, A. Brusch, D. Kolker, J.-J. Zondy, G. D. Rovera, and P. Lemonde, Phys. Rev. A **68**, 030501 (2003).
[9] C. Y. Park and T. H. Yoon, Phys. Rev. A **68**, 055401 (2003).
[10] S. G. Porsev, A. Derevianko, and E. N. Fortson, Phys. Rev. A **69**, 021403(R) (2004).
[11] S. G. Porsev, Yu. G. Rakhlina, and M. G. Kozlov, Phys. Rev. A **60**, 2781 (1999).
[12] A. Derevianko, Phys. Rev. Lett. **87**, 023002 (2001).
[13] R. G. Garstang, J. Opt. Soc. Am. **52**, 845 (1962).
[14] W. R. Johnson, K. T. Cheng, and D. R. Plante, Phys. Rev. A **55**, 2728 (1997).
[15] T. Brage, P. G. Judge, A. Aboussaid, M. R. Godefroid, P. Jon-

sson, A. Ynnerman, C. F. Fischer, and D. S. Leckrone, Astrophys. J. **500**, 507 (1998).
[16] T. Brage, P. G. Judge, and C. R. Proffitt, Phys. Rev. Lett. **89**, 281101 (2002).
[17] S. G. Porsev, M. G. Kozlov, Yu. G. Rakhlina, and A. Derevianko, Phys. Rev. A **64**, 012508 (2001).
[18] S. G. Porsev, Yu. G. Rakhlina, and M. G. Kozlov, J. Phys. B **32**, 1113 (1999).
[19] V. A. Dzuba, V. V. Flambaum, and M. G. Kozlov, Phys. Rev. A **54**, 3948 (1996).
[20] M. G. Kozlov and S. G. Porsev, Opt. Spectrosc. **87**, 384 (1999) [Opt. Spectrosc. **87**, 352 (1999)].
[21] A. Lurio, Phys. Rev. **126**, 1768 (1962).
[22] M. Arnold, E. Bergmann, P. Bopp, C. Dorsch, J. Kowalski, T. Stehlin, and F. Trager, Hyperfine Interact. **9**, 159 (1981).
[23] P. Grundevik, M. Gustavsson, I. Lindgren, G. Olsson, L. Robertsson, A. Rosen, and S. Svanberg, Phys. Rev. Lett. **42**, 1528 (1979).
[24] S. M. Heider and G. O. Brink, Phys. Rev. A **16**, 1371 (1977).
[25] D. L. Clark, M. E. Cage, D. A. Lewis, and G. W. Greenlees, Phys. Rev. A **20**, 239 (1979).
[26] B. Budick and J. Snir, Phys. Rev. **178**, 18 (1969).
[27] R. M. Sternheimer, Phys. Rev. **80**, 102 (1950).
[28] A. Dalgarno and J. T. Lewis, Proc. R. Soc. London **233**, 70 (1955).
[29] M. Yasuda and H. Katori, e-print arXive: physics/0310074.